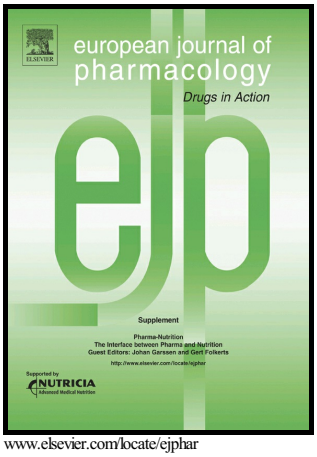

www.elsevier.com/locate/ejphar

Characterization of novel kainic acid analogs as inhibitors of select microglial functions

Morgan A. Alford, Zhenlin Tian, Frederic Menard, Andis Klegeris

PII: S0014-2999(19)30122-0
DOI: https://doi.org/10.1016/j.ejphar.2019.02.025
Reference: EJP72238

To appear in: *European Journal of Pharmacology*

Received date: 24 October 2018
Revised date: 13 February 2019
Accepted date: 14 February 2019

Cite this article as: Morgan A. Alford, Zhenlin Tian, Frederic Menard and Andis Klegeris, Characterization of novel kainic acid analogs as inhibitors of select microglial functions, *European Journal of Pharmacology,* https://doi.org/10.1016/j.ejphar.2019.02.025

Characterization of novel kainic acid analogs as inhibitors of select microglial functions

Morgan A. Alford[a], Zhenlin Tian[b], Frederic Menard[b], Andis Klegeris[a,*]

[a]Department of Biology, University of British Columbia Okanagan Campus, Kelowna, BC, Canada.

[b]Department of Chemistry, University of British Columbia Okanagan Campus, Kelowna, BC, Canada.

[*]Correspondence to: Department of Biology, University of British Columbia Okanagan Campus, 3187 University Way, Kelowna, BC V1V 1V7, Canada; andis.klegeris@ubc.ca

Abstract

Alzheimer's disease (AD) is characterized by abnormal accumulation of extracellular amyloid beta protein (Aβ) plaques and intracellular neurofibrillary tangles, as well as by a state of chronic inflammation in the central nervous system (CNS). Adverse activation of microglia, the brain immune cells, is believed to contribute to AD pathology including excessive neuronal death. Thus, normalizing immune functions of microglia could slow neurodegeneration, and identification of novel compounds capable of modifying microglial functions is an important goal. Since kainic acid (KA) has been shown to modulate microglial morphology and immune functions, we synthesized six new KA analogs (KAAs) and tested their effects on select microglial functions by using three different cell types as microglia models. Four of the KAAs at low micromolar concentrations inhibited secretion of cytotoxins, monocyte chemoattractant protein (MCP)-1, reactive oxygen species and nitric oxide (NO) by immune-stimulated microglia-like cells. We hypothesize that the effects of the novel KAAs on microglia-like cells are not mediated by KA receptors since their biological activity was distinct from that of KA in all assays performed. A structural similarity search identified aldose reductase (AR) as a potential target for the novel KAAs. This hypothesis was supported by use of AR inhibitor zopolrestat, which abolished the inhibitory effects of two KAAs on microglial secretion of NO. Since the newly developed KAAs inhibited pro-inflammatory and cytotoxic functions of

microglia, they should be further investigated for their potential beneficial effect on neuroinflammation and neurodegeneration in AD animal models.

Keywords: aldose reductase; anti-inflammatory drugs; neurodegenerative disease; neuroinflammation; neuroprotection; zopolrestat

1. Introduction

Alzheimer's disease (AD) is characterized by abnormal accumulation of amyloid beta protein (Aβ) plaques and neurofibrillary tangles; however, other pathological mechanisms, such as instability of neurotransmission and synapses, could play an early role (Frere and Slutsky, 2018). AD is characterized by a state of chronic inflammation in the central nervous system (CNS) including adverse activation of microglia, the immune cells of the brain (McKenzie et al., 2017; Takahashi et al., 2017). Over-activated microglia secrete excessive amounts of inflammatory cytokines and reactive oxygen species, which can disturb glutamatergic neurotransmission and lead to excitotoxicity (Clark and Vissel, 2017; Wang et al., 2014b). As neurons degenerate, they release factors that further activate microglia, and a cycle of chronic neuroinflammation is established.

The neuroinflammation hypothesis proposes that inflammation triggered by AD-specific molecular mechanisms drives the progression of neurodegeneration; therefore, anti-inflammatory therapies are being considered for prevention and treatment of AD (McKenzie et al., 2017, Morris et al., 2014). Numerous epidemiological studies have linked long-term use of non-steroidal anti-inflammatory drugs (NSAIDs) that inhibit cyclooxygenases to a reduced risk of developing AD (Wang et al., 2014a). However, NSAIDs have not been effective in most clinical trials (Mullane and Williams, 2012). These mixed results warrant further research to identify novel anti-inflammatory agents, with mechanisms of action different from NSAIDs, as therapeutic options for AD (Drachman et al., 2014).

Kainic acid (KA) is a naturally occurring analog of glutamate, the principal excitatory neurotransmitter in the CNS, which activates kainate receptors in neurons (Zheng et al., 2011). In microglia, KA was found to modify cell morphology (Christensen et al., 2006), as well as their expression and secretion of both pro- and anti-inflammatory cytokines and markers (Banerjee et

al., 2015; Hong et al., 2010; Zheng et al., 2010). Accordingly, we aimed to design analogs of KA that prevent adverse activation of immune-stimulated microglia. Six novel kainic acid analogs (KAAs) were synthesized and assessed for their ability to modulate select microglial functions *in vitro.* These novel KAAs differ from KA: their substituents are less polar, much larger, or both (Fig. 1). A molecular similarity search returned hits for aldose reductase (AR) inhibitors, suggesting that the KAAs reported here may share functional group complementarity to the AR active site (Mylari, 1992; Chatzopolou et al., 2014). AR is an enzyme that mediates hyperglycemia-induced oxidative stress when reducing glucose to sorbitol by producing metabolites, such as glutanionyl-1,4-dihydroxynonanol (GS-DHN), which enhance inflammation through activation of the nuclear factor (NF)-κB (Baba et al., 2013; Tang et al., 2012; Verdile et al., 2015). In the brain, AR is expressed constitutively by microglia, and is upregulated under oxidative stress. AR also detoxifies reactive aldehydes such as 3,4-dihydroxyphenylacetaldehyde, and its deficiency has been linked to Parkinson's disease (Yeung et al., 2017; Zeng et al., 2013). In the present study KAA1-4 are shown to downregulate microglial secretion of cytotoxins, monocyte chemoattractant protein (MCP)-1, reactive oxygen species and nitric oxide (NO) at low micromolar concentrations. We hypothesize that these KAAs inhibit select microglial functions by interacting with AR, and not KA receptors.

2. Materials and methods

2.1 Reagents

The following reagents were obtained from Sigma Aldrich (Oakville, ON, Canada): 3-(4,5-dimethylthiazol-2-yl)-2,5-diphenyl tetrazolium bromide (MTT), dimethyl sulfoxide (DMSO), extravidin alkaline phosphatase (#E2636), lipopolysaccharide (LPS; from *Escherichia coli* O55:B5, #L2880), luminol, *N*-(1-naphthyl)ethylenediamine dihydrochloride, *N*-formyl-Met-Leu-Phe (fMLP), phosphate buffered saline (PBS), phosphatase substrate tablets, sulfanilamide, triton X-100 and the AR inhibitor zopolrestat. KA was obtained from Tocris/Bio-Techne (Oakville, ON, Canada). Human interferon gamma (IFN-γ) and the MCP-1 enzyme-linked immunosorbent assay (ELISA) kit were purchased from Peprotech (Rocky Hill, NJ, USA). All other reagents were obtained from ThermoFisher Scientific (Ottawa, ON, Canada) unless otherwise stated.

2.2 Cell culture

THP-1 and HL-60 cell lines were purchased from the American Type Culture Collection (ATCC, Manassas, VA, USA), and the BV-2 cell line was a gift from Dr. G. Garden (University of Washington, Seattle, WA, USA). The human neuroblastoma SH-SY5Y cell line, used as a neuron model, was generously donated by Dr. R. Ross (Fordham University, Bronx, NY, USA).

All cells were grown in Dulbecco's modified Eagle medium nutrient mixture F-12 Ham (DMEM-F12) supplemented with 10% calf bovine serum (CBS) and penicillin/streptomycin x100 (PSA) (F10 medium). The cells were cultured in T-75 flasks and incubated at 37 ºC in a humidified 5% CO_2 and 95% air atmosphere. For experiments, cells were cultured in DMEM-F12 supplemented with PSA and 5% CBS (F5 medium) unless stated otherwise. All cell lines were used without differentiation, except HL-60 cells, which were treated with DMSO as described in 2.7.

2.3 Synthesis of novel kainic acid analogs (KAAs)

For general techniques, detailed experimental procedures, and complete characterization of KAA1, KAA2, KAA5, KAA6, 9-hydroxyphenylfluorenyl (PfOH), and 9-phenylfluorene (PfH) see Tian and Menard (2018). The synthesis of KAA3 and KAA4 is outlined in Fig. 1. Briefly: KAA1 (101 mg, 0.203 mmol) was hydrogenolysed using a solid-phase Pd/C catalyst (5 mg) in methanol (10 ml). The solution was degassed and charged with a hydrogen atmosphere. After 24 h, the reaction solution was filtered through a celite pad. The filtrate was concentrated to dryness under reduced pressure. The residue was triturated with methanol (15 ml) and afforded a white precipitate. The precipitate was collected by filtration to yield hydrogenated phenylfluorenyl (PfH) (47 mg, 96%) as a white solid. The filtrate was concentrated to yield KAA3 (48 mg, 92%) as a pale-yellow liquid. **KAA3**: ^{1}H NMR (400 MHz, chloroform-*d*) δ 3.98 (d, *J* = 9.7 Hz, 1H), 3.79 (s, 3H), 3.71 (s, 1H), 3.59 (d, *J* = 18.0 Hz, 1H), 3.40 (d, *J* = 18.0 Hz, 1H), 2.77–2.70 (m, 2H), 2.57-2.53 (m, 1H), 1.44 (s, 9H). KAA4 was prepared according to the procedure described for KAA3 by using KAA2 as the starting material (Fig. 1C). Using KAA2 (62 mg, 0.13 mmol) afforded KAA4 as a pale-yellow liquid (28 mg, 93%). **KAA4**: ^{1}H NMR (400 MHz, chloroform-*d*) δ 3.91 (d, *J* = 10.1 Hz, 1H), 3.87 (t, *J* = 5.4 Hz, 2H), 3.78 (s, 3H), 3.48 (d, *J* = 7.0 Hz, 1H), 3.34 (d, *J* = 7.4 Hz, 1H), 2.99 (dd, *J* = 4.7, 2.6 Hz, 1H), 2.71 (t, *J* = 5.4 Hz, 2H), 2.64 (dt, *J* = 10.6, 5.4 Hz, 2H).

2.4 THP-1 cell toxicity toward neuronal SH-SY5Y cells

Human THP-1 cells were selected as they have been shown to be good models for studying microglial cytotoxic responses and cytokine secretion (Gouveia et al., 2017; Klegeris et al., 2005). THP-1 cells were seeded into 24-well plates at a concentration of 5 x 10^5 cells/ml in one ml F5 medium. THP-1 cells were then treated with the synthetic compounds KAA1-4, KA, and PfOH (1-20 μM), or their vehicle (0.2% DMSO), 15 min prior to activation with LPS (0.2 ng/ml) plus IFN-γ (150 U/ml), or their PBS vehicle. LPS and IFN-γ were used as potent immune stimuli to model microglial activation and detect the biological activity of KAAs. At the concentration used, DMSO alone did not affect any of the parameters studied across the different cell types. Following 48 h incubation, the viability of THP-1 cells was measured using the MTT assay. Additionally, 0.5 ml of THP-1 cell supernatant were transferred onto SH-SY5Y cells, which had been plated 24 h earlier at a concentration of 2 x 10^5 cells/ml in 0.5 ml F5 medium. Following a 72 h incubation period in the THP-1 supernatants, the viability of the SH-SY5Y cells was measured by the MTT assay.

2.5 Cell viability assay

The cell viability assay measures the conversion of MTT to purple formazan by viable cells. It was performed as described previously by Hansen et al. (1989). Briefly, MTT (0.5 mg/ml) was added to cells in a 24-well plate for one h at 37 ºC under a 5% CO_2 atmosphere. Dark formazan crystals that had formed were dissolved by adding an equal volume of SDS/DMF (20% sodium dodecyl sulfate, 50% *N,N*-dimethyl formamide solution) for three h. 100 μl aliquots were transferred to 96-well plates and optical densities measured at 570 nm with a FLUOstar Omega microplate reader (BMG Labtech, Nepean, ON, Canada). The background absorbance of MTT added to cell culture media was corrected for, and data were normalized to the absorbance values from wells containing viable unstimulated control cells not exposed to any of the compounds.

2.6 Measurement of MCP-1 secretion by ELISA

ELISA was used to monitor the secretion of MCP-1, a prototypical pro-inflammatory chemotactic cytokine that is both secreted and recognized by microglia (Yang et al., 2011). THP-

1 cells were plated, treated and stimulated for 48 h as described in 2.4. MCP-1 ELISA was performed according to the manufacturer's (Peprotech) protocol.

2.7 Measurement of reactive oxygen species secretion by chemiluminescence (CHL)

Differentiated HL-60 cells were chosen to model a microglial respiratory burst response; these cells have been shown to express a high level of functional NADPH oxidase (Collins et al., 1978). A previously described chemiluminescence (CHL) assay was carried out with minor modifications (Gouveia et al., 2017). Prior to experimentation, HL-60 cells were differentiated by 1.3% DMSO in a six cm dish for five days. HL-60 cells were washed and seeded into 96-well plates at a concentration of 1 x 10^6 cells/ml in 0.25 ml phenol red-free DMEM-F12 supplemented with 2% CBS (F2 medium). HL-60 cells were treated with the synthetic KAA1-4 compounds, KA, and PfOH (1-20 μM), or their vehicle (0.2% DMSO), for 15 min prior to priming their respiratory burst response with LPS (0.5 μg/ml in PBS) for 24 h. 165 μl of the medium were removed without disturbing cells and the plates were placed in a FLUOstar Omega microplate reader. CHL intensity in each well was measured after sequential injections of luminol (10 mg/ml dissolved in PBS) and fMLP (20 μM dissolved in PBS). fMLP is an established inducer of respiratory burst response in phagocytes. Viability of HL-60 cells was assessed by the MTT assay in parallel wells as described in 2.5. CHL was quantified as described previously and the data were normalized to the signal obtained from LPS-primed and fMLP-stimulated control cells not exposed to the compounds.

2.8 Measurement of NO secretion

Murine BV-2 microglia were used to study NO secretion because this cell type has been shown to robustly respond to LPS and other inflammatory stimuli with the upregulated expression of inducible NO synthase (iNOS). BV-2 cells were seeded into 24-well plates at a concentration of 2 x 10^5 cells/ml in 0.5 ml of F5 medium and incubated for 24 h to allow for their adherence. F5 medium was replaced with a fresh aliquot and cells were treated with compounds KAA1-6, KA, and PfOH (1-20 μM), or their vehicle (0.2% DMSO), 15 min prior to activation with LPS (0.2 μg/ml), or its PBS vehicle solution. After 24 h incubation, 50 μl aliquots of cell-free BV-2 cell supernatant were transferred to 96-well plates and an equal volume of Griess reagent was added (1% sulfanilamide, 0.1% *N*-(1-napthyl)ethylenediamine

dihydrochloride, 2.5% phosphoric acid). In this assay, the Griess reagent reacts with nitrite ions, which are the stable primary breakdown products of NO, thereby causing a colorimetric change that can be measured at 550 nm (Yoshida and Kasama, 1987). Viability of the BV-2 cells was assessed by the MTT assay in parallel wells as described in 2.5.

2.9 Aldose reductase inhibition

BV-2 microglial cells were plated as described in 2.8 and incubated with the competitive AR inhibitor zopolrestat (100 μM), or its vehicle (0.05% DMSO), for 15 min. Cells were then treated with KAA1 or KAA2 (1-20 μM) for 15 min prior to activation with LPS (0.2 μg/ml), or its PBS vehicle. After 24 h incubation, 50 μl aliquots of cell-free BV-2 supernatants were transferred to 96-well plates and the Griess assay was performed. Viability of the BV-2 cells was assessed by the MTT assay in parallel wells as described in 2.5.

2.10 Statistical analysis

GraphPad Prism software (version 7.0, GraphPad Software Inc., La Jolla, CA, USA) was used to conduct statistical analyses. The randomized-block design one-way analysis of variance (ANOVA) followed by Dunnett's post-hoc test was performed to detect differences between treatment groups. Significance was established at $P < 0.05$.

3. Results

3.1 Effect of compounds on THP-1 cytotoxicity toward SH-SY5Y neuronal cells

The ability of the novel KAAs to reduce the secretion of cytotoxins by THP-1 monocytic cells was studied first. Fig. 2 shows that exposure of neuronal SH-SY5Y cells to the supernatants from THP-1 cells stimulated with LPS plus IFN-γ without KAA (0 μM) causes significant reduction in viability of neuronal cells when compared to cells exposed to supernatants from unstimulated THP-1 cells (vehicle). Treatment of THP-1 cells with KAA1-4 prior to cell stimulation with LPS and IFN-γ reduces their cytotoxicity toward SH-SY5Y cells (Fig. 2A-D). At 20 μM, KAA1-4 reduce THP-1 cytotoxicity toward SH-SY5Y cells by 83%, 72%, 64% and 73%, respectively. Fig. 2E and F demonstrate that KA and PfOH do not have significant effects on the cytotoxicity of stimulated THP-1 cells toward SH-SY5Y cells. For all concentrations studied, none of KAA1-4, KA, or PfOH affected the viability of stimulated THP-1 cells **(**Fig.

3A-F). KAA1-4 were also applied directly to SH-SY5Y cells to investigate whether they affect neuronal cell viability. At the concentrations studied (up to 20 μM), no significant effects on SH-SY5Y cell viability were observed according to the MTT assay (data not shown).

3.2 Effect of compounds on secretion of MCP-1 by THP-1 cells

Fig. 4A-D show that treatment of THP-1 cells with KAA1-4 prior to cell stimulation with LPS and IFN-γ significantly reduces secretion of MCP-1, when compared to stimulated THP-1 cells treated with the vehicle only (0 μM). The inhibitory effects of KAA1 and KAA3 are significant at 1 μM and higher, whereas KAA2 and KAA4 are inhibitory at 5 μM and 20 μM. At 20 μM, KAA1-4 reduce the concentration of MCP-1 in supernatants of stimulated THP-1 cells by 17%, 40%, 54% and 51%, respectively. Fig. 4E and 4F show that at all concentrations studied, KA and PfOH have no significant effects on the concentration of MCP-1 in supernatants of stimulated THP-1 cells. At the concentrations studied, KAA1-4, KA and PfOH do not affect the viability of stimulated THP-1 cells (Fig. 3A-F).

3.3 Effect of compounds on secretion of reactive oxygen species by primed HL-60 cells

Fig. 5A-D show that treatment of HL-60 cells with KAA1-4 prior to their priming with LPS and their stimulation with fMLP inhibits the CHL response of cells, when compared to the CHL response of LPS-primed and fMLP-stimulated HL-60 cells that have been treated with vehicle only (0 μM). KAA1 inhibits the CHL response of primed and stimulated cells at 1 μM and higher, whereas KAA2-4 are inhibitory at 5 μM and 20 μM. At 20 μM, KAA1-4 reduce the CHL response of primed and stimulated cells by 50%, 53%, 42% and 34%, respectively. At the concentrations studied, KA and PfOH have no significant effects on the CHL response of primed and stimulated cells (Fig. 5E, F). The addition of KAA1-4, KA and PfOH to LPS-primed HL-60 cells just prior to stimulation with fMLP has no significant effects on the CHL response of cells (data not shown). At the concentrations studied, KAA1-4, KA and PfOH do not affect the viability of primed and stimulated HL-60 cells (Fig. 6A-F).

3.4 Effect of compounds on secretion of NO by BV-2 microglia

Fig. 7A-D show that treatment of BV-2 microglia with KAA1-4 prior to LPS stimulation significantly inhibits the secretion of NO, when compared to the LPS-stimulated cells treated

with the vehicle only (0 μM). KAA1 and KAA3 significantly inhibit the secretion of NO by cells at 20 μM, whereas KAA2 and KAA4 are inhibitory at 5 μM and 20 μM. At 20 μM, KAA1-4 inhibit secretion of NO by 31%, 53%, 27% and 14%, respectively. At the concentrations studied, PfOH, KAA5 and KAA6 have no significant effects on the secretion of NO by BV-2 cells (Fig. 7F-H). Fig. 7E shows that treatment of BV-2 cells with 5 or 20 μM KA prior to LPS stimulation enhances NO secretion, when compared to LPS-stimulated cells treated with the vehicle only (0 μM). At the concentrations studied, KAA1-6, KA and PfOH do not affect the viability of LPS-stimulated BV-2 microglia (Fig. 8A-H). Nitrite was not detected in the supernatants of unstimulated BV-2 cells (data not shown). Detectable secretion of NO was not induced when KAA1-6, KA and PfOH were applied to BV-2 cells on their own (1 - 20 μM, data not shown).

3.5 Effect of compounds on secretion of NO by BV-2 microglia in the presence of zopolrestat

Fig. 9 illustrates that, similar to the results shown on Fig. 7, treatment of BV-2 cells with KAA1 or KAA2, prior to cell stimulation with LPS, inhibits their secretion of NO, when compared to LPS-stimulated cells treated with the vehicle only (0 μM). However, when the cells are sequentially pre-incubated with the competitive AR inhibitor zopolrestat (100 μM), then treated with KAA and stimulated with LPS, the inhibitory effects of KAA1 and KAA2 on NO secretion are abolished (Fig. 9A, B). Cell viability of LPS-stimulated BV-2 microglia was not affected by pre-incubation of cells with 100 μM zopolrestat followed by LPS-stimulation, nor by KAA1, KAA2, or zopolrestat at the studied concentrations and combinations (Fig. 10A, B).

4. Discussion

Natural kainoids that bind to KA receptors are usually neurotoxic and are therefore undesirable candidates to develop AD therapies. However, in the current study, the modifications made to the kainoid core molecule should prevent KAA1-6 from acting through KA receptors, thereby possibly eluding neurotoxic effects (Majik and Mandrekar, 2016). Indeed, the key interactions between KA and its receptors are well defined (Protein Data Bank identifier: PDB 4E0X; Krogsgaard-Larsen et al., 2015). Compounds KAA1-4 were synthesized as part of a different research program (Tian and Menard, 2018), yet their low molecular weight and desirable lipophilic characteristics suggest they may cross the blood-brain barrier. The only

conserved structural elements between the natural kainoids and the KAAs reported here are: the presence of a carboxyl group at the C2 position of the pyrrolidine ring, and a *trans* relationship between the C2-C3 substituents. The C4 alkene substituent of KA is replaced by a simple ketone (KAA1-5), or its stereochemistry is inverted (KAA6). Two of the novel analogs (KAA2 and KAA4) also differ from kainoids at the C3-side chain: the usual carboxymethyl group is replaced by a 2'-ketobutan-4'-ol sidechain. The nitrogen of the pyrrolidine core is alkylated with a large polyaromatic group (9-phenylfluorene) in four compounds (KAA1/2/5/6), making these KAAs much more hydrophobic than KA (cLogPs range from 3.4 to 6.8 in contrast to –0.6 for KA). In KAA3 and KAA4, the nitrogen can participate in hydrogen bonds and/or be protonated. Finally, compounds PfOH and PfH were tested to ensure that the observed effects are not due to inadvertent release of the polyaromatic portion of the molecules under physiological conditions; both were found to be inactive.

Based on the above structural disparity between the novel KAAs and typical kainoids, we hypothesize that the newly synthesized KAAs do not act through KA receptors. Consistent with this hypothesis, we observed that KAA1-4 are not toxic to SH-SY5Y cells at the concentrations studied. In contrast, KA is toxic to SH-SY5Y cells (Cannarsa et al., 2008). In addition, KAA1-4 compounds exhibit a biological activity different from that of KA in each of the assays performed, further supporting our hypothesis that KA receptors are not the primary target of these KAAs.

The maximal inhibition exhibited by KAA2 is superior to that of KAA1, which suggests that a relatively polar hydroxylic substituent at C3 of the pyrrolidine ring enhances the affinity of the compounds for their target. Moreover, the presence of a functional group at the C3 position and a ketone at the C4 position of the pyrrolidine ring may be essential to the biological activity of KAAs since KAA5 and KAA6 have no effect on the secretion of NO. Our data suggest that the mechanism of action may differ slightly between the compounds tested, since addition of a *N*-phenylfluorenyl group on the pyrrolidine ring of KAAs differentially modulates the inhibitory activity of KAAs on microglial secretions. For example, removal of the large, lipophilic *N*-phenylfluorenyl protecting group from KAAs enhances the inhibitory effect exhibited by the compound with an ester-containing functional group at C3 (KAA1 *versus* KAA3), but does not impact the effect exhibited by the compound with a hydroxylic substituent at the same position (KAA2 *versus* KAA4).

We hypothesized that the inhibitory activity of KAA1-4 on microglial cells is at least partially due to AR inhibition because of the structural analogy between KAA1-4 and ethyl 1-(9*H*-fluoren-9-yl)-4,5-dioxopyrrolidine-3-carboxylate, which is an established AR inhibitor (Chemical Abstracts Service identifier: 142774-45-6; Mylari, 1992). This hypothesis is supported by our data showing that the selective AR inhibitor zopolrestat abolishes the inhibitory effects of KAA1 and KAA2 on microglial NO secretion. Since AR mediates hyperglycemia-induced oxidative stress, AR inhibitors have been used clinically for treatment of complications associated with type II diabetes mellitus (Chatzopoulou et al., 2013). More recently, however, AR inhibitors have entered the research spotlight as possible therapeutics for inflammatory disorders such as rheumatoid arthritis, asthma and AD, due to findings that AR produces pro-inflammatory GS-DHN (Frohnert et al., 2014; Song et al., 2017). Consistent with our data showing the anti-inflammatory potential of KAAs due to inhibition of MCP-1 secretion, previous studies have demonstrated that AR inhibitors reduce the secretion of two other inflammatory cytokines, tumor necrosis factor (TNF)-α and interleukin (IL)-1β, by BV-2 cells, RAW264.7 macrophages or retinal microglia (Chang et al., 2014; Song et al., 2017; Zeng et al., 2013). AR activity has been linked to activation of NF-κB as well as upregulated microglial secretion of MCP-1, reactive oxygen species and NO (Ramana et al., 2004; Song et al., 2017; Zeng et al., 2013), indicating that the inhibitory effects of KAAs may include downregulation of NF-κB activity in microglia.

KAA1-4 described in this study have the potential to slow down neuroinflammation in AD by inhibiting microglial cytotoxicity, secretion of MCP-1, reactive oxygen species and NO. MCP-1 can be secreted by microglia in response to tissue lesions to promote the chemotaxis of monocytes and other glial cells toward the site of injury for mounting an immune response (Azizi et al., 2015; Clark and Vissel, 2017). In diseased brains, however, over-activated microglia secrete MCP-1 at high concentrations that augment the deposition of Aβ plaques and worsen AD pathology (Porcellini et al., 2013). Reactive oxygen species production is increased in AD due to age-related mitochondrial deterioration and microglial activation (Wang et al., 2014b). High concentrations of reactive oxygen species hinder a broad spectrum of cellular processes, which may cause further cellular damage and exacerbation of AD-associated neurodegeneration. NO is yet another important CNS messenger that has been implicated in the progression of AD when produced at high concentrations (Azizi et al., 2015; Balez and Ooim,

2015). The expression of iNOS, which is the enzyme that produces NO, is upregulated in microglia exposed to harmful stimuli such as Aβ. NO causes direct neurotoxicity, similarly to reactive oxygen species, by disrupting mitochondrial integrity (Azizi et al., 2015; Wang et al., 2014b).

Elevated levels of NO (Yuste et al., 2015), reactive oxygen species (Cruz-Haces et al., 2017) and inflammatory cytokines (Viviani et al., 2014) have also been linked to enhanced excitotoxicity, thereby increasing neuronal death indirectly. Excitotoxicity involves excessive activation of the neuronal *N*-methyl-D-aspartate (NMDA) receptors by glutamate leading to a large calcium influx, which causes loss of mitochondrial and nuclear functions as well as activation of calcium-dependent proteases (Meldrum and Garthwaite, 1990). Excitotoxicity is facilitated by microglial NO and reactive oxygen species blocking the reuptake of glutamate, which increases its concentration in the synaptic cleft (Cruz-Haces et al., 2017; Yuste et al., 2015). High levels of inflammatory cytokines facilitate glutamate release from glial cells and enhance excitotoxic neuronal death by modulating the expression, phosphorylation and activity of NMDA receptors (Viviani et al., 2014).

By inhibiting secretion of cytotoxins and several different microglial inflammatory mediators, the newly synthesized KAA1-4 have the potential to reduce neuronal death in neurodegenerative diseases, including AD, which have a strong neuroinflammatory component; however, further preclinical studies will be required to establish this activity in AD animal models. Further *in vivo* testing of the novel KAAs is especially important, as microglial populations are heterogeneous and they display functional diversity along spatial and temporal axes (Hanisch, 2013). This could lead to potentially competing physiological effects: the activation of certain microglial subtypes may be detrimental, while activation of other subtypes could be beneficial for CNS homeostasis. Current *in vitro* models of microglial activation cannot reliably predict clinically beneficial modulators since the gene expression patterns in these different microglia subtypes are not well characterized at the single-cell level (Silvin and Ginhoux, 2018). Recent experiments using PLX5622, an inhibitor of colony-stimulating factor 1 receptor that depletes microglia, further illustrate the opposite roles that microglia sometimes play in neuropathologies. For example, depletion of microglia can avert plaque deposition and cognitive decline in AD animal models (Dagher et al., 2015; El-Gamal et al., 2018), or prevent disruption of the blood-retina barrier during chronic inflammation induced by LPS (Kokona et

al., 2018), but it is detrimental in viral encephalitis (Waltl et al., 2018) and prion disease (Carroll et al., 2018). Pharmacological modulators of microglia functions may have drastically different clinical effects in neuropathologies depending on the overall role neuroinflammation and microglia play in each specific case. We posit that the compounds reported herein provide new tools to investigate the complex functions of microglia in neurodegenerative pathologies.

5. Conclusions

Dysregulated microgliosis contributes to neuroinflammation and neurotoxicity; therefore, therapeutics that attenuate the adverse activation of microglia could be used to slow down the progression of AD. In a search for small molecules that can regulate microglial immune functions, we synthesized a series of compounds based on the core structure of KA. We studied their effects in three different microglia cell models: THP-1, HL-60 and BV-2 cells, which were chosen due to their robust responses in four different functional assays measuring secretion of cytotoxins, the chemokine MCP-1, reactive oxygen species and NO. We show that four of the eight compounds tested inhibit the above microglial functions at low micromolar concentrations. By using a selective AR inhibitor we show that the inhibitory action of bioactive KAAs is at least partially mediated by this enzyme. Such inhibitory effects on microglia can have an indirect beneficial outcome on neuron survival. Thus, KAA1-4 identified herein may represent novel candidate molecules for future preclinical studies aimed at developing anti-AD therapeutics.

Funding support

This work was supported by grants from the Natural Sciences and Engineering Research Council of Canada (NSERC), the Jack Brown and Family Alzheimer's Disease Research Foundation and the University of British Columbia (UBC) Okanagan campus.

Conflict of interest

The authors have declared that there is no conflict of interest.

References

Azizi, G., Navabi, S., Al-Shukaili, A. Seyedzadeh, M.H., Yazdani, R., Mirshafiey A. 2015. The role of inflammatory mediators in the pathogenesis of Alzheimer's disease. Sultan Qaboos Univ. Med. J. 15, 305-316. doi: 10.18295/squmj.2015.15.03.002

Baba, S.P., Hoetker, J.D., Merchant, M., Klein, J.B., Cai, J., Barski, O.A., Conklin, D.J., Bhatnagar, A. 2013. Role of aldose reductase in the metabolism and detoxification of carosine-acrolein conjugates. J. Biol. Chem. 288, 28163-28179. doi: 10.1074/jbc.M113.504753

Balez, R., Ooim, L. 2015. Getting to NO Alzheimer's disease: neuroprotection versus neurotoxicity mediated by nitric oxide. Oxid. Med. Cell. Longev. 1, 1-8. doi: 10.1155/2016/3806157

Banerjee, M., Sasse, V.A., Wang, Y., Maulik, M., Kar, S. 2015. Increased levels and activity of cathepsins B and D in kainate-induced toxicity. Neuroscience 22, 360-373. doi: 10.1016/j.neuroscience.2014.10.003

Cannarsa, R., Landuzzi, D., Cavina, C., Candeletti, S., Romualdi, P. 2008. Kainic acid downregulated NOP receptor density and gene expression in human neuroblastoma SH-SY5Y cells. J. Mol. Neurosci. 35, 171-177. doi: 10.1016/j.neuint.2012.02.015

Carroll, J.A., Race, B., Williams, K., Striebel, J., Chesebro, B. 2018. Microglia are critical in host defence against prion disease. J. Virol. Epub 29769333 doi: 10.1128/JVI.00549-18

Chang, K.C., Ponder, J., LaBarbera, D.V., Petrash, J.M. 2014. Aldose reductase inhibition prevents endotoxin-induced inflammatory responses in retinal microglia. Invest. Ophthalmol. Vis. Sci. 55, 2853-2861. doi: 10.1167/iovs.13-13487

Chatzopoulou, M., Pegklidou, K., Papastavrou, N., Demopoulos, V.J. 2013. Development of aldose reductase inhibitors for the treatment of inflammatory disorders. Exp. Opin. Drug Discov. 8, 1365-1380. doi: 10.1517/17460441.2013.843524

Chatzopoulou, M., Parsilinakos, A., Vallianatou, T., Prnova, M.S., Zakelj, S., Ragno, R., Stefek, M., Kristl, A., Tsantili-Kakoulidou, A., Demopoulos, V.J. 2014. Decreasing acidity in a series of aldose reductase inhibitors: 2-fluoro-4-(1H-pyrrol-1-yl)phenol as a scaffold for improved membrane permeation. Bioorganic. Med. Chem. 22, 2194-2207. doi: 10.1016/j.bmc.2014.02.016

Christensen, R.N., Ha, B.K., Bresnahan, J.C., Beattie, M.S. 2006. Kainate induces rapid redistribution of the actin cytoskeleton in ameboid microglia. J. Neurosci. Res. 84, 170-181. doi: 10.1002/jnr.20865

Clark, I. A., Vissel, B. 2017. The meteorology of cytokine storms, and the clinical usefulness of this knowledge. Sem. Immunopathology 39, 505-516. doi: 10.1007/s00281-017-0628-y

Collins, S.J., Ruscetti, F.W., Gallagher, R.E., Gallo, R.C. 1978. Terminal differentiation of human promyelocytic leukemia cells induced by dimethyl sulfoxide and other polar compounds. Proc. Natl. Acad. Sci. U.S.A. 75, 2458-2462

Cruz-Haces, M., Tang, J., Acosta, G., Fernandez, J., Shi, R. 2017. Pathological correlations between traumatic brain injury and chronic neurodegenerative diseases. Transl. Neurodegener. 6, 20. doi: 10.1186/s40035-017-0088-2

Dagher, N.N., Najafi, A.R., Kayala, K.M., Elmore, M.R., White, T.E., Medeiros, R., West, B.L., Green, K.N. 2015. Colony-stimulating factor 1 receptor inhibition prevents microglial plaque association and improves cognition in 3xTg-AD mice. J. Neuroinflam. 12: 139, 1-14. doi: 10.1186/s12974-015-0366-9

Drachman, D.A. 2014. The amyloid hypothesis, time to move on: amyloid is the downstream result, not cause, of Alzheimer's disease. Alz. Dementia 10, 372-380. doi: 10.1016/j.jalz.2013.11.003

El-Gamal, M.I., Al-Ameen, S.K., Al-Koumi, D.M., Hamad, M.G., Jalal, N.A., Oh, C.H. 2018. Recent advances of colony-stimulating factor-1 receptor (CSF-1R) kinase and its inhibitors. J. Med. Chem. 61, 5450-5466. doi: 10.1021/acs.jmedchem.7b00873

Frere, S., Slutsky, I. 2018. Alzheimer's disease: From firing instability to homeostasis network collapse. Neuron 97**,** 32–58. doi: 10.1016/j.neuron.2017.11.028

Frohnert, B.I., Long, E.K., Hahn, W.S., Bernlohr, D.A. 2014. Glutathionated lipid aldehydes are products of adipocyte oxidative stress and activators of macrophage inflammation. Diabetes 63, 89-100. doi: 10.2337/db13-0777

Gouveia, A., Bajwa, E., Klegeris, A. 2017. Extracellular cytochrome C as an intercellular signaling molecule regulating microglial functions. Biochim. Biophys. Acta 1861(9): 2274-2281. doi: 10.1016/j.bbagen.2017.06.017

Hanisch, U.K. 2013. Functional diversity of microglia – how heterogeneous are they to begin with? Front. Cell. Neurosci. 7: 65, 1-18. doi: 10.3389/fncel.2013.00065

Hansen, M.B., Nielsen, S.E., Berg, K. 1989. Re-examination and further development of a precise and rapid dye method for measuring cell growth/cell kill. J. Immunol. Methods 119, 203-210.

Hong, J., Cho, I.H., Kwak, K. I., Suh, E. C., Seo, J., Min, H. J., Choi, S. Y., Kim, C. H., Park, S. H., Jo, E. K., Lee, S., Lee, K. E., Lee, S. J. 2010. Microglial toll-like receptor 2 contributes to kainic acid-induced glial activation and hippocampal neuronal death. J. Biol. Chem. 285, 39447-39457. doi: 10.1074/jbc.M110.132522

Klegeris, A., Bissonnette, C. J., McGeer, P.L. 2005. Modulation of human microglia and THP-1 cell toxicity by cytokines endogenous to the nervous system. Neurobiol. Aging 26, 673-682. doi: 10.1016/j.neurobiolaging.2004.06.012

Kokona, D., Ebneter, A., Escher, P., Zinkernagel, M.S. 2018. Colony-stimulating factor 1 receptor inhibition prevents disruption of the blood-retina barrier during chronic inflammation. J. Neuroinflam. 25: 340. doi: 10.1186/s12974-018-1373-4

Krogsgaard-Larsen, N., Storgaard, M., Møller, C., Demmer, C.S., Hansen, J., Han, L., Monrad R.N., Nielsen, B., Tapken, D., Pickering, D.S., Kastrup, J.S., Frydenvang, K., Bunch, L. 2015. Structure-activity relationship study of ionotropic glutamate receptor antagonist (2*S*,3*R*)-3-(3-carboxyphenyl)pyrrolidine-2-carboxylic acid. J. Med. Chem. 58, 6131-6150. doi: 10.1021/acs.jmedchem.5b00750

Majik, M., Madrekar, K. 2016. Recent progress in syntheses and biological activities of kainic acid and its derivatives. Curr. Org. Chem. 20, 939-951. doi: 10.2174/13852728 19666150804000728

McKenzie, J.A., Spielman, L.J., Pointer, C.B., Lowry, J.R., Bajwa, E., Lee, C.W., Klegeris, A. 2017. Neuroinflammation as a common mechanism associated with the modifiable risk factors for Alzheimer's and Parkinson's diseases. Curr. Aging Sci. 10, 158-176. doi: 10.2174/1874609810666170315113244.

Meldrum, B., Garthwaite, J. 1990. .Excitatory amino acid neurotoxicity and neurodegenerative disease. Trends Pharmacol. Sci. 11, 379−387. doi: 10.1016/0165-6147(90)90184-A

Morris, G.P., Clark, I.A., Vissel, B. 2014. Inconsistencies and controversies surrounding the amyloid hypothesis of Alzheimer's disease. Acta Neuropathol. Commun. 2, 1-21. doi: 10.1186/s40478-014-0135-5

Mullane, K., Williams, M. 2012. Alzheimer's therapeutics: continued clinical failures question the validity of the amyloid hypothesis- but what lies beyond? Biochem. Pharmacol. 85, 289-305. doi: 10.1016/j.bcp.2012.11.014

Mylari, B.L. 1992. Preparation of pyrrolidinedionecarboxylates as aldose reductase inhibitors. PCT Int. Appl. Patent no: *WO 9206954 A2 19920430*

Porcellini, E., Ianni, M., Carbone, I., Francheschi, M., Licastro, F. 2013. Monocyte chemoattractant protein-1 promoter polymorphism and plasma levels in Alzheimer's disease. Immun. Ageing 10, 1-6. doi: 10.1186/1742-4933-10-6

Ramana, K.V., Friedrich, B., Srivastava, S., Chatnagar, A., Srivastava, S.K. 2004. Activation of nuclear factor-kappaB by hyperglycemia in vascular smooth muscle cells is regulated by aldose reductase. Diabetes 53, 2910-2920. doi: 10.2337/diabetes.53.11.2910

Silvin, A., Ginhoux, F. 2018. Microglia heterogeneity along a spatio-temporal axis: more questions than answers. Glia 66, 2045-2057. doi: 10.1002/glia.23458

Song, X.M., Yu, Q., Dong, X., Yang, H.O., Zeng, K.W., Li, J.,Tu, P.F. 2017. Aldose reductase inhibitors attenuate β-amyloid induced TNF-α production in microglia via ROS-PKC-mediated NF-κB and MAPK pathways. Int. Immunopharmacol. 50, 30-37. doi: 10.1016/j.intimp.2017.06.005

Takahashi, R.H., Nagao, T., Gouras, G.K. 2017. Plaque formation and the intraneuronal accumulation of β-amyloid in Alzheimer's disease. Pathol. Int. 67, 185-193. doi: 10.1111/pin.12520

Tang, W.H., Martin, K.A., Hwa, J. 2012. Aldose reductase, oxidative stress, and diabetic mellitus. Front. Pharmacol. 3, 87-95. doi: 10.3389/fphar.2012.00087

Tian, Z., Menard, F. 2018. Synthesis of kainoids and C4 derivatives. J. Org. Chem. 83, 6162-6170. doi: 10.1021/acs.joc.8b00179

Verdile, G., Keane, K.N., Cruzat, V.F., Medic, S., Sabale, M., Rowles, J., Wijesekara, N., Martins, R.N., Fraser, P.E., Newsholme, P. 2015. Inflammation and oxidative stress: the molecular connectivity between insulin resistance, obesity and Alzheimer's disease. Mediators Inflamm. 1, 1-17. doi: 10.1155/2015/105828

Viviani, B., Boraso, M., Marchetti, N., Marinovich, M. 2014. Perspectives on neuroinflammation and excitotoxicity: a neurotoxic conspiracy? Neurotoxicology 43, 10-20. doi: 10.1016/j.neuro.2014.03.004.

Waltl, I., Kaufer, C., Gerhauser, I., Chhatbar, C., Ghita, L., Klinke, U., Loscher, W. 2018. Microglia have a protective role in viral encephalitis-induced seizure development and hippocampal damage. Brain Behav. Immun. 74, 186-204. doi: 10.1016/j.bbi.2018.09.006

Wang, J., Tan, L., Wang, H.F., Tan, C.C., Meng, X.F., Wang, C., Tang, S.W., Yu, J.T. 2014a. Anti-inflammatory drugs and risk of Alzheimer's disease: an updated systematic review and meta-analysis. J. Alzheimer Dis. 44, 385-396. doi: 10.3233/jad-141506

Wang, X., Wang, W., Li, L., Perry, G., Lee, H. G., Zhu, X. 2014b. Oxidative stress and mitochondrial dysfunction in Alzheimer's disease. Biochim. Biophys. Acta 1842, 1240-1247. doi: 10.1016/jbbadis.2013.10.015

Yang, G., Meng, Y., Li, W., Yong, Y., Fan, Z., Ding, H., Wei, Y., Luo, J., Ke, Z.J. 2011. Neuronal MCP-1 mediates microglia recruitment and neurodegeneration induced by the mild impairment of oxidative metabolism. Brain Pathol. 21, 279-297. doi: 10.1111/j.1750-3639.2010.00445.x

Yeung, P.K.K., Lai, A.K.W., Son, H.J., Zhange, X., Hwang, O., Chung, S.S.M., Chung, S.K. 2017. Aldose reductase deficiency leads to oxidative stress-induced dopaminergic neuronal loss and autophagic abnormality in an animal model of Parkinson's disease. Neurobiol. Aging 50, 119-133. doi: 10.1016/j.neurobiolaging.2016.11.008

Yoshida, K., Kasama, K. 1987. Biotransformation of nitric oxide. Environ. Health Perspect. 73, 201-206.

Yuste J.E., Tarragon, E., Campuzano, C.M., Ros-Bernal, F. 2015. Implications of glial nitric oide in neurodegenerative diseases. Front. Cell. Neurosci. 9, 322. doi: 10.3389/fncel.2015.00322

Zeng, K.W., Li, J., Dong, X., Wang, Y.H., Ma, Z.Z., Jiang, Y., Jin, H.W., Tu, P.F. 2013. Anti-neuroinflammatory efficacy of the aldose reductase inhibitor FMHM via phospholipase C/ protein kinase C-dependent NF-κB and MAPK pathways. Toxicol. Appl. Pharmacol. 273(1), 159-171. doi: 10.1016/j.taap.2013.08.028

Zheng, H., Zhu, W., Zhao, H., Wang, X., Wang, W., Li, Z. 2010. Kainic acid-activated microglia mediate increased excitability of rat hippocampal neurons in vitro and in vivo: crucial role of interleukin-1 beta. Neuroimmunomodulation 17, 31-38. doi: 10.1159/000243083

Zheng, X.Y., Zhang, H.L., Luo, Q., Zhu, J. 2011. Kainic acid-induced neurodegenerative model: potentials and limitations. J. Biomed. Biotechnol. 457079, 1-10. doi: 10.1155/2011/457079

Figure 1. Structures of the compounds tested and synthesis of KAA3 and KAA4. (A) Compounds KAA1-6, KA, PfOH and PfH. KAA1/3/5/6, PfH and PfOH were synthesized as previously reported (Tian and Menard, 2018). **(B)** KAA3 was synthesized by removing the Pf group from KAA1. **(C)** KAA4 was synthesized by removing the Pf group from KAA2. Abbreviations used: Dess-Martin periodinane (DMP), dichloromethane (DCM), hexamethylphosphoramide (HMPA), hydrogenated protecting group (PfH), hydroxylated protecting group (PfOH), kainic acid (KA), kainic acid analog (KAA), *meta*-chloroperoxybenzoic acid (*m*CPBA), *n*-butyllithium (*n*BuLi), palladium/carbon catalyst (Pd/C); protecting group (Pf), *tert*-butyl (tBu), *tert*-butyldimethylsilyl (TBS), tetrahydrofuran (THF).

Figure 2. KAA1-4 inhibit the toxicity of stimulated human monocytic THP-1 cells toward SH-SY5Y cells. THP-1 cells were treated with KAA1-4 **(A-D)**, KA **(E)**, PfOH **(F)** or their vehicle (0.2% DMSO) for 15 min. Cells were then stimulated with LPS (0.2 ng/ml) & IFN-γ (150 U/ml) as indicated on the abscissa. Following 48 h incubation, THP-1 cell supernatant was transferred to SH-SY5Y cells. Following 72 h exposure to the THP-1 cell supernatants, SH-SY5Y cell viability was assessed by the MTT assay. Data from four independent experiments are presented as mean % of the control cell viability ± standard error of the mean (SEM). Control cells were treated with fresh F5 media instead of THP-1 cell supernatant (data not shown). ***** $P < 0.05$, ** $P < 0.01$ different from vehicle-treated, stimulated cells (0 μM) according to the randomized block one-way ANOVA followed by Dunnett's post-hoc test. P and F values for the main effects of the ANOVA are shown on the graphs.

Figure 3. At the concentrations studied, compounds do not affect the viability of stimulated human monocytic THP-1 cells. Cells were treated with KAA1-4 **(A-D)**, KA **(E),** PfOH **(F)** or their vehicle (0.2% DMSO) for 15 min. THP-1 cells were then stimulated with LPS (0.2 ng/ml) & IFN-γ (150 U/ml) as shown on the abscissa. Following 48 h incubation, THP-1 cell viability was assessed by the MTT assay. Data from four independent experiments are presented as mean % of the unstimulated control cell viability ± SEM. Unstimulated control cells were seeded in the absence of KAAs and solvent (data not shown). ***** $P < 0.05$ different from vehicle-treated, stimulated cells (0 μM) according to the randomized block one-way ANOVA followed by

Dunnett's post-hoc test. P and F values for the main effects of ANOVA are shown on the graphs.

Figure 4. KAA1-4 reduce the concentration of MCP-1 in the supernatants of stimulated human monocytic THP-1 cells. Cells were treated with KAA1-4 **(A-D)**, KA **(E)**, PfOH **(F)** or their vehicle (0.2% DMSO) for 15 min. THP-1 cells were then stimulated with LPS (0.2 µg/ml) & IFN-γ (150 U/ml). MCP-1 (ng/ml) was measured in THP-1 cell supernatants following 48 h incubation. Data from four independent experiments are presented as means ± SEM. ***** $P < 0.05$, ** $P < 0.01$ different from vehicle-treated, stimulated cells (0 µM) according to the randomized block one-way ANOVA followed by Dunnett's post-hoc test. P and F values for the main effects of ANOVA are shown on the graphs. The limit of detection of the ELISA is displayed as a dashed line at 1.1 ± 0.2 ng/ml.

Figure 5. KAA1-4 inhibit reactive oxygen species secretion by primed and stimulated human HL-60 cells in a concentration-dependent manner. DMSO-differentiated cells were treated with KAA1-4 **(A-D)**, KA **(E)**, PfOH **(F)** or their vehicle (0.2% DMSO) for 15 min and then primed with LPS (0.5 µg/ml). Following 24 h incubation, the cells were stimulated with fMLP (1 µM) and the luminol-dependent chemiluminescence (CHL) was measured. Data from four independent experiments are presented as mean % CHL intensity of the primed and stimulated control HL-60 cells ± SEM. Control HL-60 cells were seeded in the absence of compounds and solvent (data not shown). ***** $P < 0.05$, ** $P < 0.01$ different from vehicle-treated, stimulated cells (0 µM) according to the randomized block one-way ANOVA followed by Dunnett's post-hoc test. P and F values for the main effects of ANOVA are shown on the graphs.

Figure 6. At the concentrations studied, compounds do not affect the viability of primed and stimulated human HL-60 cells. Cells were treated with KAA1-4 **(A-D)**, KA **(E)**, PfOH **(F)** or their vehicle (0.2% DMSO) for 15 min and then primed with LPS (0.2 µg/ml). Following 24 h incubation, HL-60 cell viability was assessed by the MTT assay. Data from four independent experiments are presented as mean % of the primed unstimulated control cell viability ± SEM. Control cells were primed with LPS but seeded in the absence of compounds and solvent (data not shown). No treatment groups were different from vehicle-treated, stimulated cells (0 µM) according to the randomized block one-way ANOVA followed by Dunnett's post-hoc test. P and

F values for the main effects of ANOVA are shown on the graphs.

Figure 7. **KAA1-4 reduce nitrite concentration in the supernatant of stimulated murine BV-2 microglia.** Cells were treated with KAA1-4 **(A-D)**, KA **(E)**, PfOH **(F)**, KAA5 **(G)**, KAA6 **(H)** or their vehicle (0.2% DMSO) for 15 min and then stimulated with LPS (0.2 µg/ml). Following 24 h incubation, nitrite (µM) was measured in cell supernatants. Data from four independent experiments are presented as means ± SEM. ***** $P < 0.05$, ** $P < 0.01$ different from vehicle-treated, stimulated cells (0 µM) according to the randomized block one-way ANOVA followed by Dunnett's post-hoc test. P and F values for the main effects of ANOVA are shown on the graphs. The limit of detection of the Griess assay is displayed as a dashed line at 1.2 ± 0.3 µM.

Figure 8. At the concentrations studied, compounds do not affect the viability of stimulated murine BV-2 microglia. Cells were treated with KAA1-4 **(A-D)**, KA **(E)**, PfOH **(F),** KAA5 **(G)**, KAA6 **(H)** or their vehicle (0.2% DMSO) for 15 min and then stimulated with LPS (0.2 µg/ml). Following 24 h incubation, BV-2 cell viability was assessed by the MTT assay. Data from four independent experiments are presented as mean % of the unstimulated control cell viability ± SEM. Unstimulated control cells were seeded in the absence of compounds and solvent (data not shown). No statistically significant effects were observed according to the randomized block one-way ANOVA. P and F values for the main effects of ANOVA are shown on the graphs.

Figure 9. Zopolrestat abolishes the effects of KAA1 and KAA2 on nitrite secretion by stimulated murine BV-2 microglia. BV-2 cells were preincubated with zopolrestat (100 µM) or its vehicle (0.05% v/v DMSO) for 15 min. Cells were then treated with KAA1 **(A)**, KAA2 **(B)** or their vehicle (0.2% v/v DMSO) for 15 min and stimulated with LPS (0.2 µg/ml). Following 24 h incubation, the concentration of nitrite (µM) was measured in cell supernatants by the Griess assay. Data from five independent experiments are presented as means ± SEM. The randomized block one-way ANOVA and Dunnett's post-hoc test were used to determine the effects of KAA treatment in the presence or absence of zopolrestat. ***** $P < 0.05$, ** $P < 0.01$ different from vehicle-treated, stimulated cells (0 µM). P_1 and F_1 values for the main effect of KAA treatment

alone, and P_2 and F_2 values for the main effect of KAA treatment in the presence of zopolrestat.. The limit of detection of the Griess assay is displayed as a dashed line at 0.9 ± 0.7 μM.

Figure 10. At the concentrations studied, zopolrestat in combination with KAA1 or KAA2 does not affect the viability of stimulated murine BV-2 microglia. Cells were preincubated with zopolrestat (100 μM) or its vehicle (0.05% v/v DMSO) for 15 min. Cells were then treated with KAA1 **(A)**, KAA2 **(B)** or their vehicle (0.2% v/v DMSO) for 15 min and stimulated with LPS (0.2 μg/ml). Following 24 h incubation, BV-2 cell viability was assessed by the MTT assay. Data from five independent experiments are presented as mean % of the unstimulated control cell viability ± SEM. Control cells were seeded in the absence of compounds and solvent (data not shown). According to the randomized block one-way ANOVA, there were no significant effects of KAA in the presence or absence of zopolrestat. P_1 and F_1 values for the main effect of KAA treatment alone, and P_2 and F_2 values for the main effect of KAA treatment in the presence of zopolrestat.

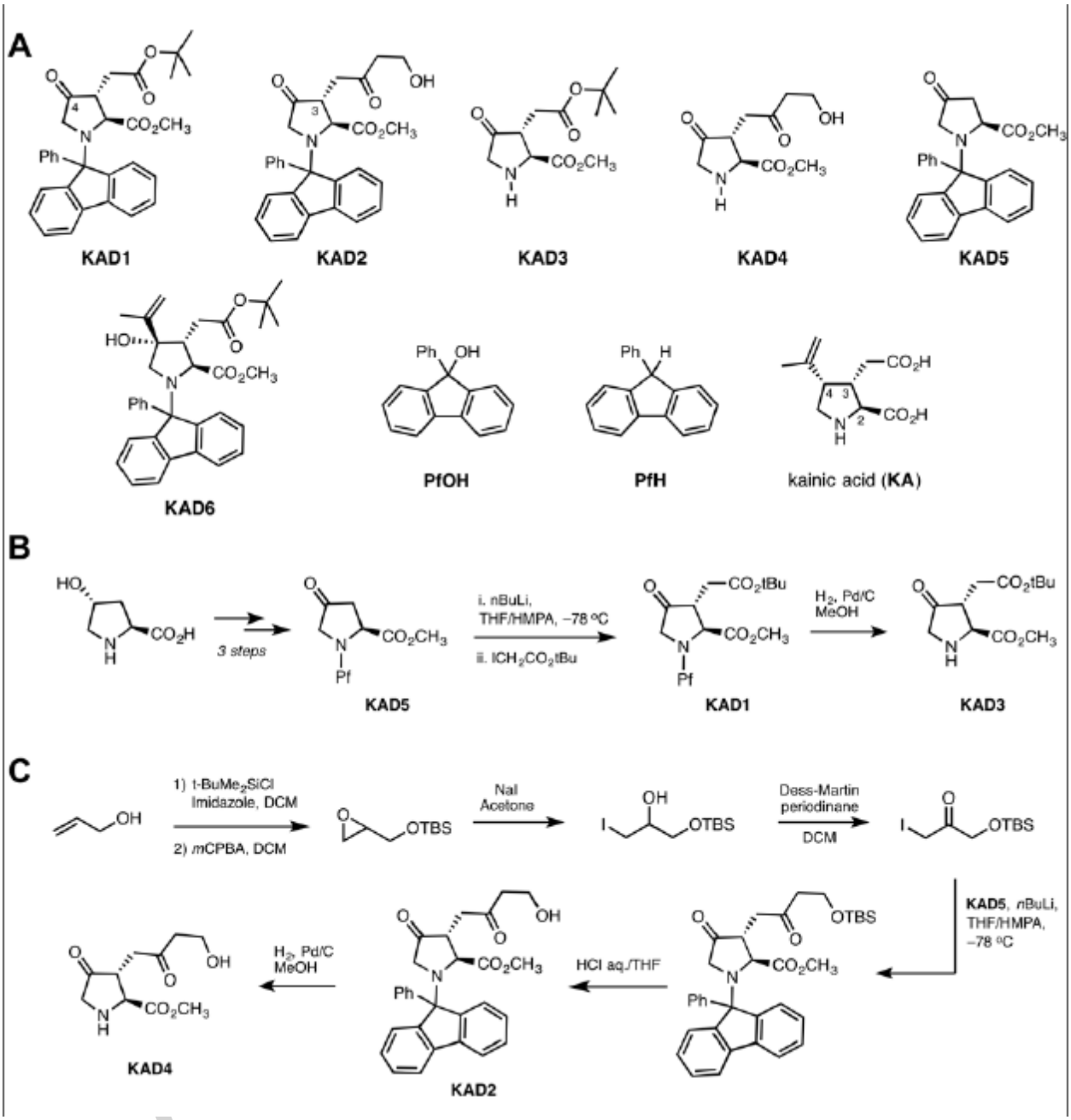
A
KAD1
KAD2
KAD3
KAD4
KAD5
KAD6
PfOH
PfH
kainic acid (KA)
B
3 steps
KAD5
i. nBuLi, THF/HMPA, −78 °C
ii. ICH2CO2tBu
KAD1
H2, Pd/C MeOH
KAD3
C
1) t-BuMe2SiCl Imidazole, DCM
2) mCPBA, DCM
NaI Acetone
Dess-Martin periodinane DCM
KAD5, nBuLi, THF/HMPA, −78 °C
HCl aq./THF
H2, Pd/C MeOH
KAD2
KAD4

Fig. 1.

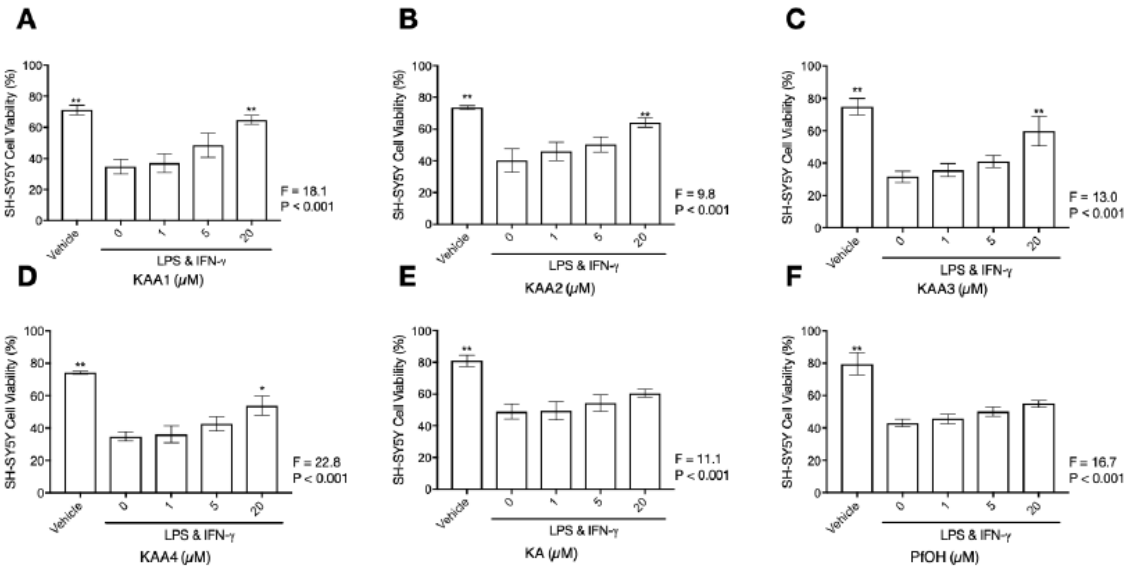

Fig. 2.

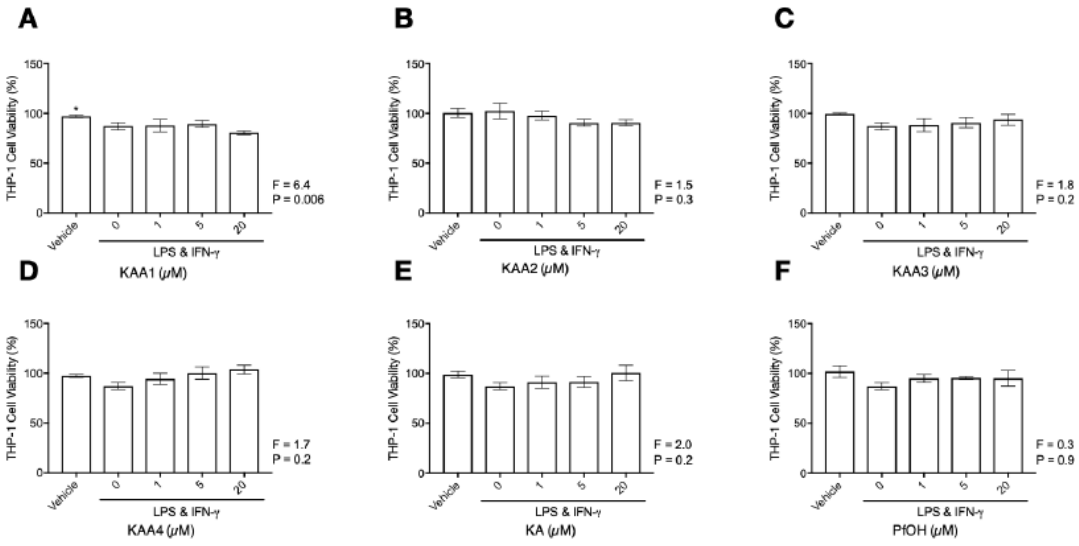

Fig. 3.

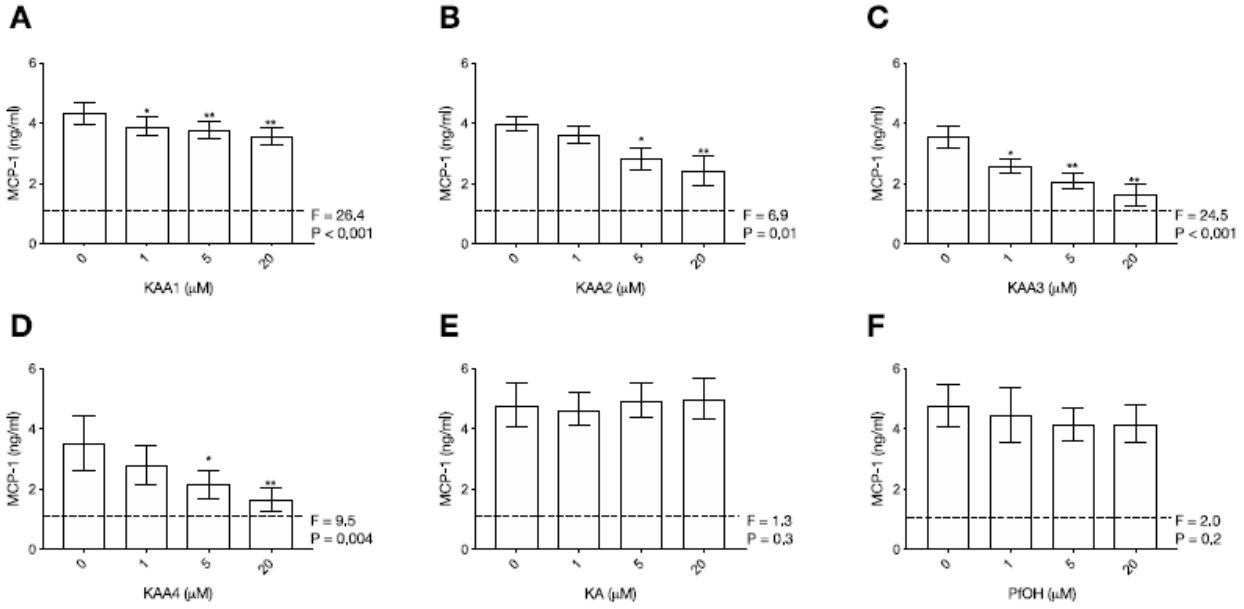

Fig. 4.

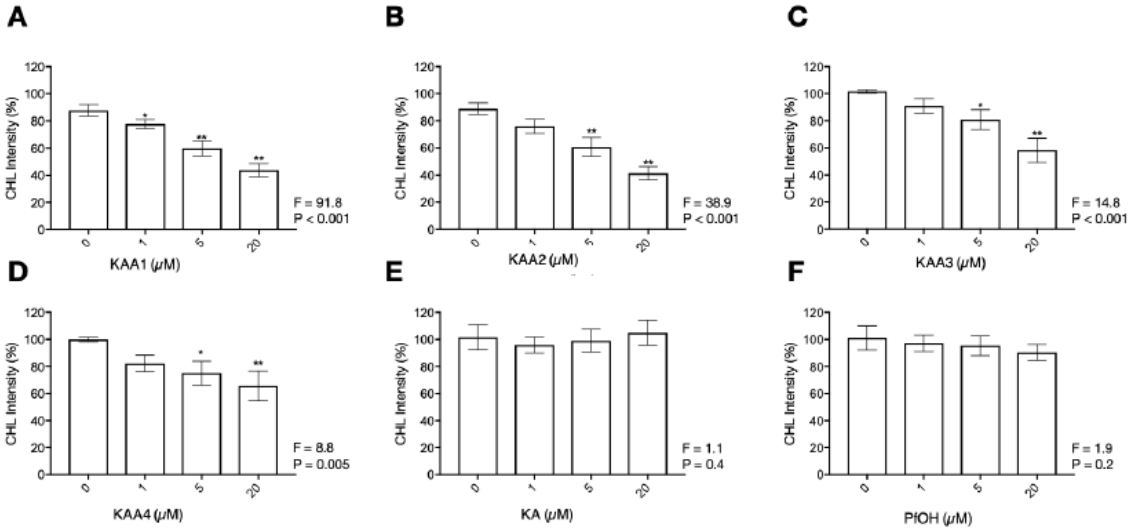

Fig. 5.

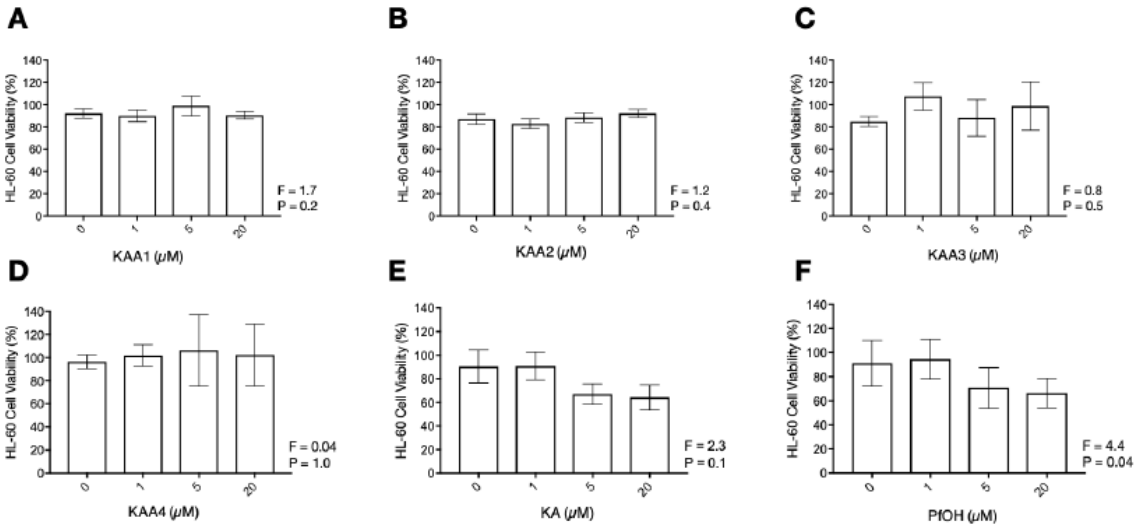

Fig. 6.

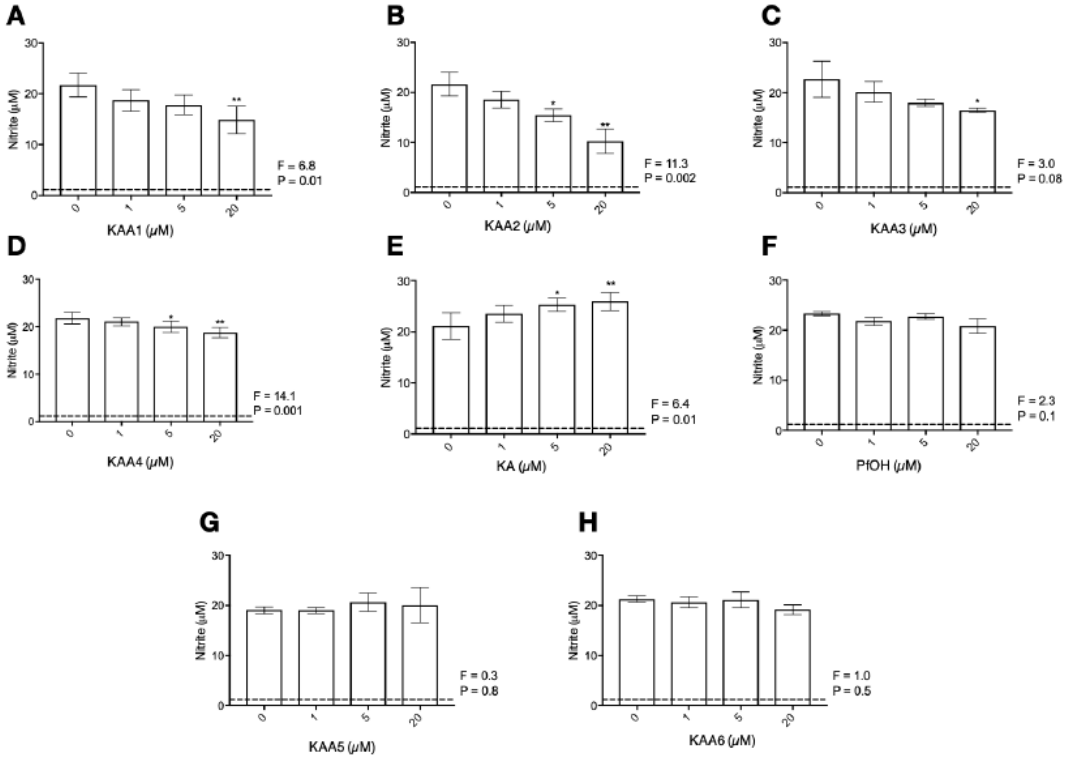

Fig. 7.

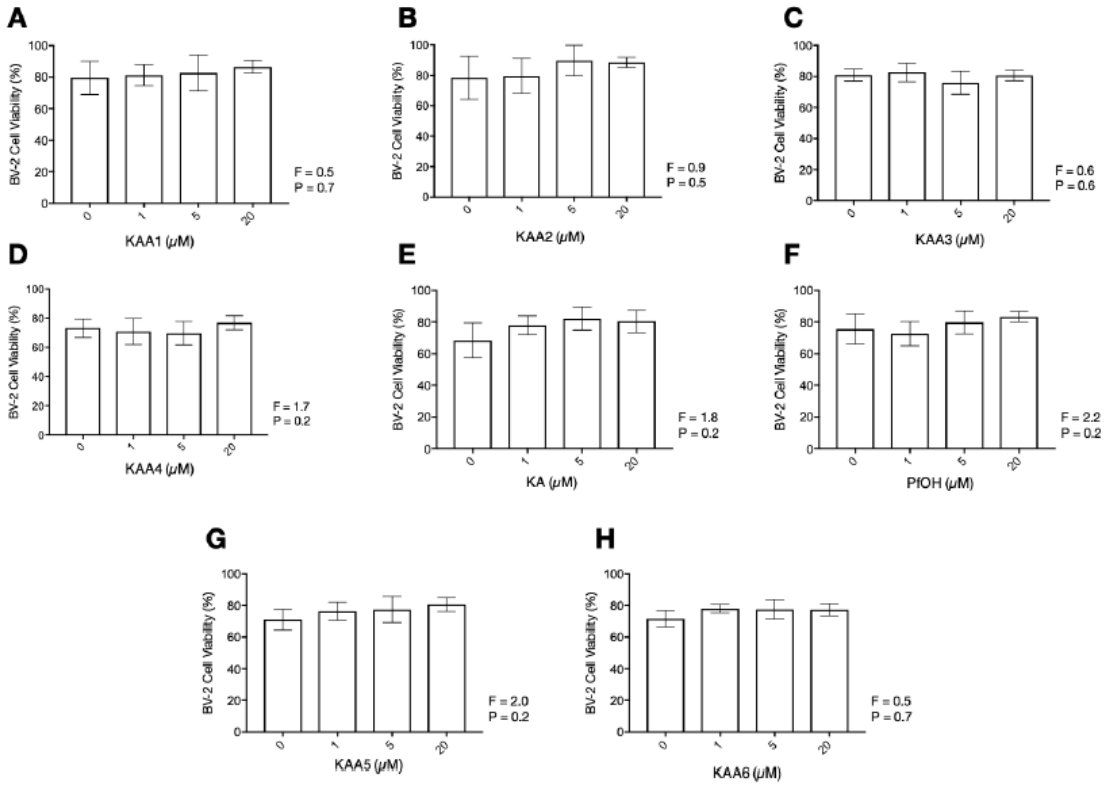

Fig. 8.

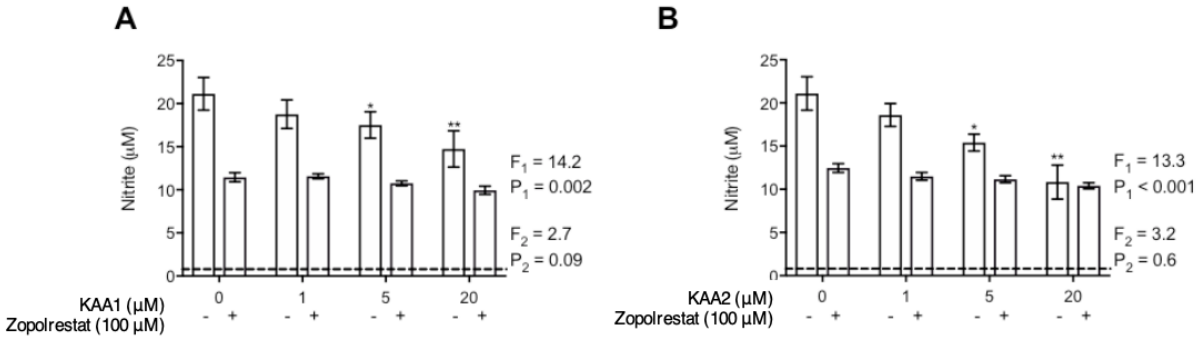

Fig. 9.

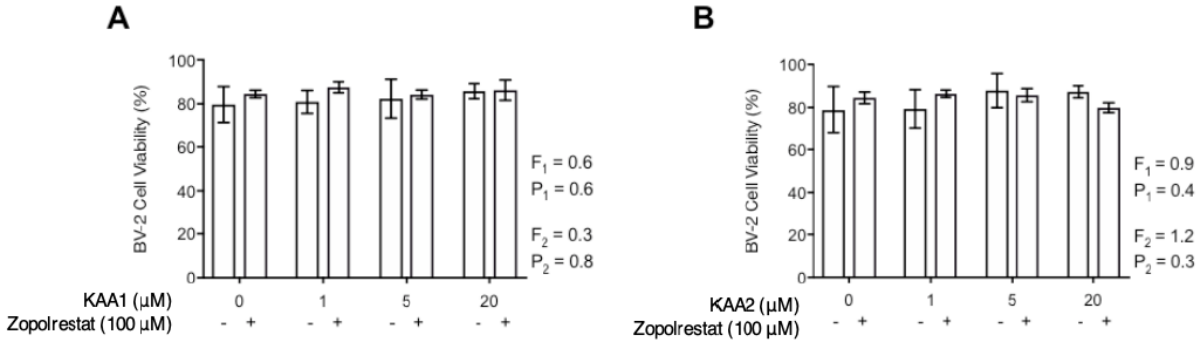

Fig. 10.